Bulletin of Electrical Engineering and Informatics
Vol. 15, No. 2, April 2026, pp. 1494~1508
ISSN: 2302-9285, DOI: 10.11591/eei.v15i2.8674

Evaluating the effectiveness of digital filtering techniques in electronic stethoscopes: a study of Kalman and Butterworth filters

Endang Dian Setioningsih[1], Sumber[1], Triwiyanto[1], Vugar Abdullayev[2], Farid Amrinsani[1], Bima Maulana Raharjo[1], Tetrik Fa'altin[1]
[1]Department of Electromedical Engineering, Poltekkes Kemenkes, Surabaya, Indonesia
[2]Department of Computer Engineering, Azerbaijan State Oil and Industry University, Baku, Azerbaijan

Article Info

Article history:

Received May 8, 2024
Revised Dec 12, 2025
Accepted Feb 22, 2026

Keywords:

Butterworth band-pass filter
Condenser microphone
Kalman filter
Mannequin heart sound
Signal-to-noise ratio

ABSTRACT

Heart sound, or phonocardiogram (PCG), signals are often distorted by noise from respiration, movement, and the surrounding environment, which complicates accurate cardiac feature extraction in portable monitoring systems. This study aims to design and evaluate an effective digital filtering method to enhance PCG signal quality obtained from a low-cost acquisition system based on a condenser microphone sensor and an ESP32 microcontroller. The main contribution of this work is the implementation and comparison of two noise-reduction approaches: Butterworth band-pass filters of various orders and the Kalman filter applied to PCG signals acquired from mannequin-based simulations. Data were recorded for 10 seconds at a 1000 Hz sampling rate, processed in MATLAB, and analyzed using the fast Fourier transform (FFT) to determine the optimal frequency ranges. Experimental results demonstrate that the 8th-order Butterworth band-pass filter achieved the highest signal-to-noise ratio (SNR) improvement, averaging 25.659 dB, outperforming other configurations. These findings indicate that an appropriately tuned Butterworth filter provides a simpler yet robust solution for real-time PCG denoising in embedded systems. Future work will integrate the filtering process directly into the ESP32 firmware and evaluate its performance on human subjects to enhance clinical applicability.

Corresponding Author:

Sumber
Department of Electromedical Engineering, Poltekkes Kemenkes Surabaya
St. Pucang Jajar Timur No. 10, Surabaya, 60245, Indonesia
Email: sumber72@poltekkesdepkes-sby.ac.id

1. INTRODUCTION

Cardiovascular disease (CVD) remains one of the leading causes of morbidity and mortality worldwide and is the primary cause of death in Indonesia [1]-[4]. Heart disease occurs when the cardiac system experiences structural or functional abnormalities [5], which may include problems involving the coronary blood vessels, heart rhythm, cardiac covering, or congenital conditions [6]. Many cardiac disorders are reflected in the acoustic characteristics of heart sounds, making cardiac auscultation (the act of listening to these sounds) an essential diagnostic method for early detection of cardiovascular abnormalities [7]-[9]. The stethoscope, as a noninvasive and affordable diagnostic device, enables medical practitioners to assess cardiac function through auscultation [10], [11]. However, the interpretation of heart sounds remains subjective and depends heavily on the physician's experience and hearing sensitivity [12], [13].

Despite continuous advancements in electronic stethoscope technology, significant challenges persist in accurately capturing and interpreting heart sounds due to ambient noise interference and the limitations of traditional acoustic amplification. Conventional stethoscopes amplify sound mechanically, which makes them vulnerable to environmental disturbances, reducing diagnostic accuracy [14], [15]. The condenser microphone sensor, commonly used in low-cost electronic stethoscopes, features automatic gain control (AGC) for dynamic sound capture but remains sensitive to external noise sources. Thus, the use of robust digital filtering techniques is essential to enhance the signal-to-noise ratio (SNR) and ensure that primary heart sound components (S1 and S2) are clearly preserved [16], [17].

Several researchers have proposed digital filtering methods to improve the quality of electronic stethoscope recordings. Wu *et al.* [18] implemented a 4^{th}-order digital Butterworth band-pass filter (20–400 Hz), effectively reducing high-frequency noise while maintaining S1 and S2 clarity, but the system performed poorly under nonstationary noise. Zhang *et al.* [19] developed an AI-assisted electronic stethoscope using a Butterworth pre-filter followed by a convolutional neural network (CNN) for classification, improving diagnostic accuracy but revealing that static filters alone were inadequate against variable acoustic interference. Zhu *et al.* [20] reviewed phonocardiogram (PCG) processing methods and highlighted Kalman filters as robust alternatives to Butterworth filters for non-stationary noise, albeit with increased computational complexity. Nugraha *et al.* [21] compared Butterworth and Kalman filters in cardiac monitoring, finding that Butterworth filters preserved waveform morphology and were computationally efficient, while Kalman filters achieved higher SNR in noisy environments. Malwade *et al.* [22] developed a Bluetooth-based digital stethoscope capable of transmitting heart sounds in real time to Bluetooth speakers or headsets, though the study did not include further signal analysis. In related work, Kjeldsen *et al.* [23] employed the condenser microphone sensor and Arduino to detect heart rate and compared data transmission using an auxiliary cable and Bluetooth. The results showed minimal differences between the two transmission modes; however, their system did not incorporate any digital filtering stage. Overall, existing studies highlight the potential of electronic stethoscopes but reveal persistent noise interference and the limited use of digital filtering, particularly for the condenser microphone sensor. Since heart sound frequencies typically range between 20 Hz and 500 Hz, this range can serve as the basis for determining suitable cutoff frequencies in filter design to improve signal clarity and analysis accuracy.

Although adaptive filtering approaches such as least mean square (LMS), recursive least squares (RLS), and wavelet-based denoising have been widely applied in biomedical signal enhancement [24], their adoption in embedded stethoscope systems remains limited. These adaptive filters can dynamically adjust their coefficients to track signal variations, making them suitable for nonstationary environments. However, their high computational and memory demands pose challenges for resource-constrained microcontrollers such as the ESP32, which is commonly used in portable biomedical devices [25]. Moreover, adaptive filters require extensive parameter tuning and large datasets to ensure convergence and stability, which are not applicable to controlled mannequin-based simulations used in this study. Therefore, despite their theoretical advantages, adaptive techniques are less practical for low-power embedded implementations, where efficiency and real-time performance are critical. Previous studies have not systematically compared the performance of Butterworth and Kalman filters—two well-established yet computationally feasible algorithms—on embedded hardware using the condenser microphone sensor. This gap motivates the present work.

Based on the research described above, the electronic stethoscope offers many advantages but is still affected by noise interference that influences sound detection results, as well as by the limited application of digital filters on the condenser microphone sensor used as the electronic stethoscope's front-end transducer. The signals are processed through an ESP32-based microcontroller, transmitted to a personal computer (PC) for visualization, and output to a Bluetooth headset for real-time auscultation. Overall, the lowest frequency range of heart sounds starts from 20 Hz to 500 Hz, which can serve as the basis for determining the cutoff frequency range of the digital filter applied to the condenser microphone module. The process of analyzing the effectiveness of digital filter usage in a stethoscope using the condenser microphone module can influence the final results of the frequency analysis displayed.

a. This study introduces a comparative analysis of Kalman and Butterworth digital filters applied to PCG signals acquired using the condenser microphone sensor, providing empirical insights into their noise-reduction effectiveness and computational suitability for embedded stethoscope systems.
b. The research demonstrates that the 8^{th}-order Butterworth band-pass filter achieves the highest average SNR improvement (25.659 dB), outperforming the Kalman filter and establishing an optimal frequency range (20–150 Hz) for heart sound enhancement in low-cost electronic stethoscopes.
c. This work contributes a practical implementation framework for integrating digital filtering algorithms into ESP32-based biomedical devices, offering a foundation for future real-time firmware development and clinical validation of electronic stethoscope systems.

Based on this, the references above still lack an analysis of electronic stethoscope development. Therefore, the authors planned to design an electronic stethoscope using the condenser microphone sensor module as a heart sound transducer, which will be processed using the ESP32 microcontroller, and compare the use of the Kalman filter with the Butterworth band-pass filter as digital filters to determine the most effective approach. The results of signal processing using digital filters will be transmitted to a PC and can be listened to through a Bluetooth headset. In this case, the use of the condenser microphone sensor is analyzed for its effectiveness when combined with the Kalman digital filter and the Butterworth band-pass filter. The two results are further compared using the SNR value method to examine their differences, and the filtered signals are transmitted to the Bluetooth headset for auditory comparison.

2. MATERIALS AND METHOD

2.1. Experimental setup

This study used mannequins with a normal sinus rhythm mode as subjects for heart sound data collection. Heart sounds were recorded from each mannequin 15 times. After acquisition using an electronic stethoscope, the signal was displayed on PC for further processing with two types of digital filters: the Kalman filter and the Butterworth band-pass filter implemented in MATLAB. The detected heart sound signals were also transmitted to a Bluetooth headset for listening purposes.

2.1.1. Materials and tools

The study utilized the condenser microphone sensor, an electret condenser microphone with built-in AGC and a frequency response of 20–20,000 Hz, to capture heart sounds from mannequins. The ESP32 microcontroller was used for signal acquisition and wireless data transmission, while MATLAB served as the primary platform for signal filtering and analysis. Two digital filtering methods were applied:

a. Kalman filter, implemented using a one-dimensional state-space model to estimate the true signal from noisy measurements. The process noise covariance (Q) and measurement noise covariance (R) were empirically tuned across several configurations (R:100 Q:1, R:10 Q:1, R:1 Q:1, and R:1 Q:0.1) to analyze their effects on SNR performance.
b. Butterworth band-pass filter, designed with cutoff frequencies of 20–150 Hz, determined empirically from fast Fourier transform (FFT) analysis of the raw PCG signals and consistent with previous studies [26]. Filter orders of 2, 4, 6, and 8 were evaluated to examine the trade-off between noise reduction and signal distortion.

A Bluetooth headset was used to receive the output sound captured by the sensor in real time.

2.1.2. Experiment

After assembling the system, experiments were conducted on 10 mannequins in the normal sinus rhythm mode. Each heart sound signal was recorded for 10 seconds with a sampling frequency of 1000 Hz. The condenser microphone sensor was positioned on the chest area of each mannequin, and data collection was performed in a quiet laboratory environment by a single operator to ensure measurement consistency and minimize ambient noise. The acquired signals were transmitted from the ESP32 to the PC, where FFT analysis was used to verify the dominant frequency range (20–150 Hz). Subsequently, each signal was processed using both the Kalman and Butterworth filters under their respective parameter settings, and the output was evaluated based on the SNR improvement before and after filtering.

2.2. The diagram block

Figure 1 describes the block diagram of the system. In the block diagram, there are three main sections: input, process, and output. The input section of the stethoscope captures the sound of the human heart. The chest piece vibrations of the stethoscope are detected by the condenser microphone sensor, and once the sound is received, the heart sound data are processed by the ESP32 microcontroller. In the ESP32, the data are filtered using digital filters, namely the Kalman filter and the Butterworth band-pass filter, which aim to clarify the heart sound signal within a specific frequency range.

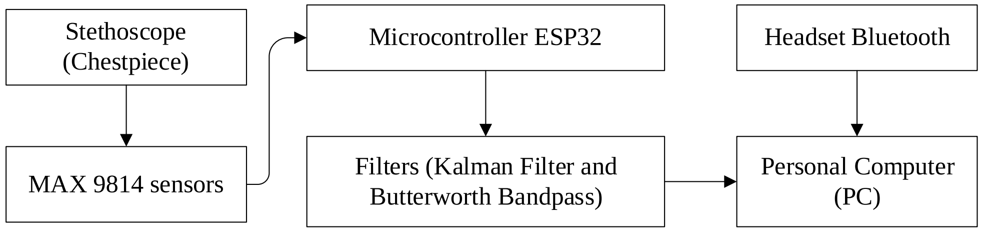

Figure 1. The diagram block of the electronic stethoscope

2.3. The flowchart

Figure 2 describes the program flow diagram. When the device is turned on, the heart rate is detected by the condenser microphone sensor, and the signal is sent to the ESP32 for data processing. The heart sound data detected by the sensor are then transmitted to the MATLAB application, where they are processed using two different types of filters, namely the Kalman filter and the Butterworth band-pass filter. Based on the results of these two filters, the SNR value is obtained and analyzed.

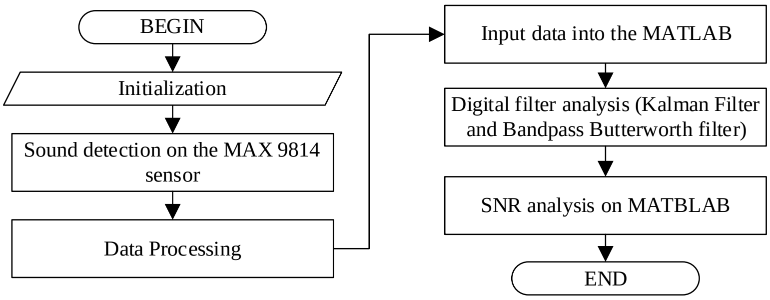

Figure 2. Program flowchart of the electronic stethoscope

Figure 3 illustrates the complete signal processing flow implemented in this study. The process begins with the acquisition of PCG signals using the condenser microphone sensor connected to the ESP32 microcontroller at a sampling rate of 1000 Hz. The collected data are transmitted to a PC for preprocessing, including normalization, trimming, and FFT analysis to determine the dominant frequency range (20–150 Hz). The signal is then processed using two filtering techniques: the Butterworth band-pass filter and the Kalman filter. After filtering, the SNR is calculated, and the results from both methods are compared in the time and frequency domains to evaluate filtering performance.

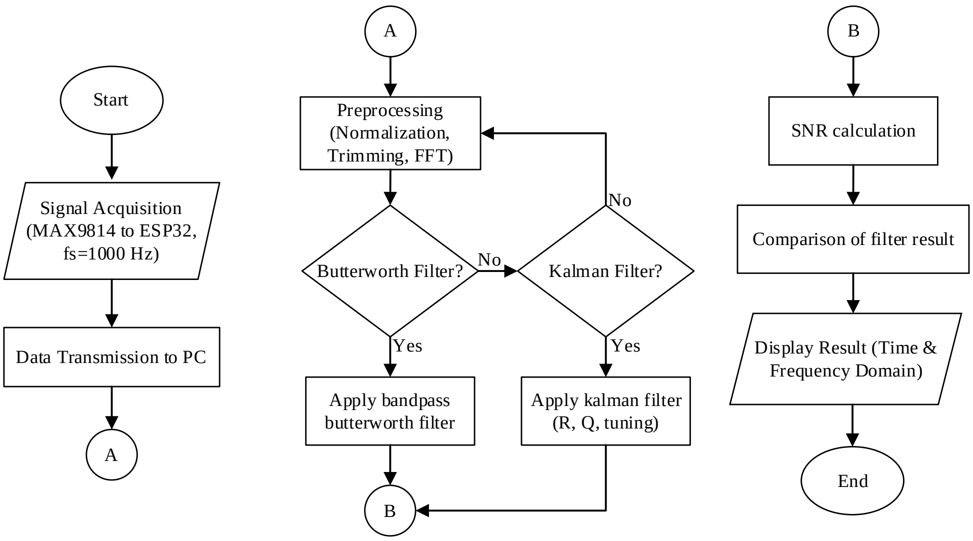

Figure 3. Flowchart of PCG signal processing and filtering pipeline

2.4. Data processing

2.4.1. Butterworth band-pass filter

In this study, a digital Butterworth band-ass filter designed in the MATLAB application was used. This digital band-pass filter was applied to reduce or eliminate noise that occurs during data acquisition using the module. The filter works by reducing or removing noise below the lower cutoff frequency (Fc1), passing the desired frequency components, and then attenuating signals above the upper cutoff frequency (Fc2). The sampling frequency used in this Butterworth band-pass digital filter is 1000 Hz, with a cutoff frequency range of 20–150 Hz. The filter orders used in this Butterworth band-pass digital filter are the 2^{nd} order, 4^{th} order, 6^{th} order, and 8^{th} orders.

a. Analog Butterworth prototype

The design of a Butterworth analog filter begins with the normalized low-pass prototype, characterized by a cutoff angular frequency of $\omega c = 1\, rad/s$). The poles S_k of the normalized $n-th$ Butterworth filter are located uniformly on the left half of the unit circle in the complex $s-plane$ and are defined as (1):

$$S_k = e^{j\pi\frac{2k+n-1}{2n}}, \text{ k=1,2, ….. ,n.} \tag{1}$$

These satisfy $sk = 1$ and $\Re\,(s_k) < 0$ ensuring system stability and a maximally flat magnitude response in the passband. The normalized analog transfer function $H_a(s)$ can be expressed as (2):

$$H_a(s) = \frac{B_0}{\prod_{k=1}^{n}(s-s_k)} \tag{2}$$

where B_0 is chosen so that $|H_a(0)| = 1$ providing a unity DC gain for the low-pass filter. For the normalized prototype, $B_0 = (-1^n)\ \prod_{k=1}^{n} s_k$ which results in a real constant. This normalization facilitates easier frequency scaling and transformation for high-pass, band-pass, and band-stop filter designs.

b. Frequency scaling (real cutoff)

In practical filter design, the normalized Butterworth prototype with a cutoff frequency of $\omega c = 1\, rad/s$ must often be scaled to meet a desired real cutoff frequency, Ω_c, this process is known as frequency scaling. To achieve the specified cutoff, the poles of the normalized transfer function are scaled according to (3):

$$p_k = \Omega_c \cdot s_k \tag{3}$$

where s_k are the normalized poles and p_k are the scaled poles corresponding to the desired cutoff frequency. Consequently, the analog transfer function of the scaled Butterworth filter becomes (4):

$$H_a(s) = \frac{B}{\prod_{k=1}^{n}(s-p_k)} \tag{4}$$

with B is a constant selected to achieve the desired DC gain, which is typically normalized to unity for low-pass filters. This scaling ensures that the filter maintains its Butterworth characteristics—specifically, a maximally flat magnitude response in the passband—while shifting the cutoff frequency to the required value.

c. Mapping to digital: bilinear transform+prewarping

Designing a digital IIR Butterworth filter typically uses the bilinear transform. It is calculated as (5):

$$s \leftarrow \frac{2}{T}\frac{1-z^{-1}}{1+z^{-1}} \text{ or } s = \frac{2}{T}\frac{z-1}{z+1} \tag{5}$$

where $T = 1/f_s$ is the sampling period and f_s is sampling frequency.

Prewarping

Because the bilinear transform warps frequency, prewarp the desired discrete cutoff frequency f_c(Hz) into the analog domain. It calculated as (6):

$$\Omega_c = 2f_s \tan(\frac{\pi f_c}{f_s}) \tag{6}$$

use radians/sec for Ω_c. Design the analog prototype with this Ω_c then apply the bilinear transform.

The process of designing a digital filter using the bilinear transformation begins by determining the filter order n, sampling frequency f_s and digital cutoff frequency f_c. Next, the prewarped analog cutoff frequency is calculated as $\Omega c = 2f_s \tan(\ \pi f_c/f_s)$ to compensate for frequency distortion introduced by the bilinear transformation. The normalized prototype poles s_k are then computed and scaled using $p_k = \Omega_c \cdot s_k$. The analog transfer function is formed as $H_a(s) = B/\prod_{k=1}^{n}(s-s_k)$ with the constant B adjusted so that $H_a(0)$=1. The transformation from the analog to the digital domain is achieved by substituting $s = \frac{2}{T}\frac{1-z^{-1}}{1+z^{-1}}$ into $H_a(s)$. The result is then multiplied by $(1+z^{-1})$ to obtain a rational function in terms of z^{-1} expressed as $H(z) = \frac{B(z)}{A(z)}$. Finally, the digital coefficients $b_0, \dots\dots, b_n$ and $a_{0\,,\dots\dots,} a_n$ are extracted, typically normalized so that $a_{0=1}$.

d. Digital transfer function and difference equation

After substitution and rearrangement. It calculated as (7):

$$H(z) = \frac{b_{0+b1z^{-1}+\cdots+bnz^{-n}}}{a_{0+a1z^{-1}+\cdots+anz^{-n}}} \quad (7)$$

commonly scaled so $a_0 = 1$. The time-domain difference equation for implementation is (8):

$$y[n] = \sum_{k=1}^{n} aky[n-k] + \sum_{k=0}^{n} bkx[n-k] \quad (8)$$

In (8) represents the time-domain implementation of the digital Butterworth filter, which defines how the output signal y[n] is computed based on both the current and previous input samples x[n-k], as well as previous output samples y[n-k]. In this equation, bk are the feedforward coefficients derived from the numerator of the digital transfer function, while ak are the feedback coefficients obtained from the denominator, typically normalized so that. The variable $n$denotes the filter order, which determines the number of past samples used in the computation. The term $\sum b_k x[n-k]$ represents the weighted contribution of current and past input samples, while $\sum a_k y[n-k]$ accounts for the recursive feedback from previously filtered outputs. This recursive structure characterizes an infinite impulse response (IIR) filter, allowing it to produce a smooth and continuous response with fewer coefficients compared to non-recursive finite impulse response (FIR) filters.

2.4.2. Kalman filter

In this study, a Kalman filter-type digital filter was used. The purpose of using the Kalman filter digital filter is to reduce noise that enters the data acquisition process using modules [27]. This filter works by obtaining the gain value set in the Kalman filter formula, which has been modified as (9):
Predict is calculated as (9):

$$\begin{aligned} \hat{x}_{t|t-1} &= \hat{x}_{t-1|t-1} \\ P_{t|t-1} &= P_{t-1|t-1} + Q_t \end{aligned} \quad (9)$$

Update is calculated as (10):

$$\begin{aligned} K_t &= P_{t|t-1}(P_{t|t-1}H^T + R_t)^{-1} \\ \hat{x}_{t|t} &= \hat{x}_{t|t-1} + K_t(y_t - H\hat{x}_{t|t-1}) \\ P_{t|t} &= (I - K_t)_{|t-1} \end{aligned} \quad (10)$$

To change the gain in the Kalman filter, the coefficient value was adjusted with the following combinations: R=100; Q=1, R=10; Q=1, R=1; Q=1, and R=1; and Q=0.1 RQ [27]. The variables in the Kalman filter equations represent the key components of the recursive estimation process. The term $\hat{x}_{t|t-1}$ denotes the predicted state estimate at time t based on information available up to the previous step, while $\hat{x}_{t|t}$ represents the updated or corrected state estimate after incorporating the current measurement y_t. The matrices $P_{t|t-1}$ and $P_{t|t}$ correspond to the predicted and updated error covariances, respectively, indicating the uncertainty associated with each estimate. K_t is the Kalman gain, which determines the weighting between the model prediction and the new measurement; a higher K_t gives more importance to the measurement data. Q_t and R_t represent the process noise covariance and measurement noise covariance, which control the filter's sensitivity and responsiveness to variations in the signal and noise levels. H is the observation matrix that maps the true state space into the measurement domain, while I denotes the identity matrix used to maintain the dimensional consistency of the covariance update. Together, these parameters enable the Kalman filter to iteratively refine its estimation of the true signal by minimizing the mean squared error between the predicted and observed values.

2.4.3. Signal-to-noise ratio

SNR is a measure used in signal analysis that compares the desired signal level to the background noise level. It is defined as the ratio of signal power to noise power and is often expressed in decibels (dB). The higher the SNR value, the better the signal quality. The SNR value can be calculated using a formula that relates signal strength to noise, as shown in (11):

$$Ps = \frac{1}{N}\sum_{i=1}^{N}|x_i|^2 \quad (11)$$

In the expression $P_s = \frac{1}{N}\sum_{i=1}^{N} \mid x_i \mid^2$, the variable P_s denotes the average power of the discrete-time signal, representing the mean energy per sample over the observation window; N is the total number of samples considered, defining the length of the discrete signal segment or analysis window; i is the summation index, an integer counter that runs from 1 to N, used to reference each individual sample in the sequence; x_i is the value of the signal at the i-th sample, which may be real- or complex-valued depending on the signal domain; and $\mid x_i \mid^2$ is the squared magnitude of the sample, corresponding to the instantaneous energy contribution of that sample, where for real signals it reduces to x_i^2, and for complex signals it is computed as $x_i x_i^*$, with x_i^* being the complex conjugate of x_i. To find out the noise value (n), it is necessary to know the frequency of noise in the heart signal. The noise signal is at the output frequency of the heart sound signal (20-150 Hz). The noise frequency of the recording signal. Furthermore, (i) is the amplitude of the signal at a time. It is calculated as (12):

$$Pn = \frac{1}{N}\sum_{i=1}^{N}|n_i|^2 \qquad (12)$$

After that, we find the Pn value or mean square value of the noise amplitude. N is the number of samples in the signal and is the amplitude of noise at a time (i) obtained from the noise frequency of the Nn_i heart sound. Broadly speaking, itis the sum of the squares of the entire amplitude of absolute noise from time (i) the number of samples on the signal. Then we can enter the variables Ps and Pn into the SNR formula, namely; $y{:}\sum_{i=1}^{N}|n_i|^2$:

$$SNR\ (dB) = 10log_{10}\frac{Ps}{Pn} \qquad (13)$$

In the expression (13), the variable $SNR_{(dB)}$ denotes the signal-to-noise ratio expressed in decibels, providing a logarithmic measure of signal quality that facilitates comparison across wide dynamic ranges; P_s represents the average power of the useful signal component, typically obtained as the mean squared magnitude of the signal samples over a defined observation interval; P_n denotes the average power of the noise component, calculated analogously as the mean squared magnitude of the noise samples; the ratio $\frac{P_s}{P_n}$ is a dimensionless linear quantity indicating how many times stronger the signal is relative to the noise; the constant factor 10 arises from the definition of decibels for power quantities (as opposed to 20 for amplitude ratios); and $\log_{10}(\cdot)$ is the base-10 logarithm, which maps multiplicative power ratios into additive decibel values, enabling more convenient interpretation and analysis in signal processing systems.

3. RESULTS AND DISCUSSION

In this study, the electronic stethoscope was tested using the condenser microphone sensor, and the measurement results were displayed on a PC for analysis in the MATLAB application. The device output could also be listened to using a Bluetooth headset. Figure 4 shows the circuit design inside the enclosure.

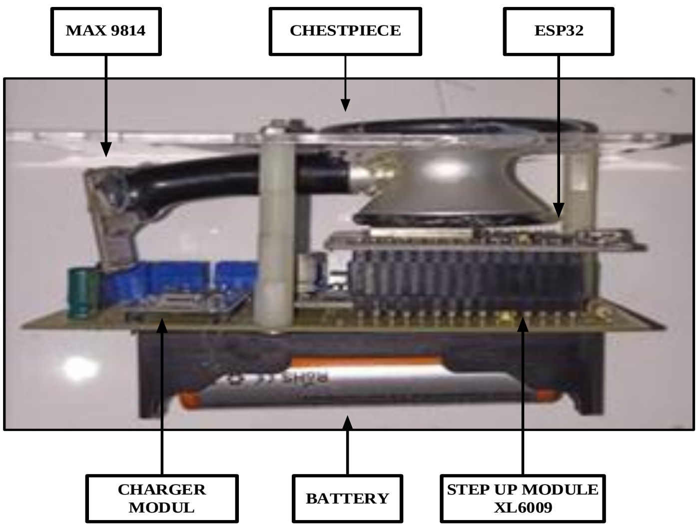

Figure 4. Design of the circuit in the enclosure (Box)

3.1. Signal-to-noise ratio measurement of the signal after the digital filter

Figures 5 and 6 illustrate the time- and frequency-domain responses of the PCG signals before and after digital filtering. In the time domain, both filters successfully reduce baseline noise; however, the Kalman filter produces a smoother output with reduced amplitude peaks, indicating slight attenuation of the primary heart sound components. Conversely, the Butterworth filter (20–150 Hz) maintains the shape and intensity of S1–S2 waves while effectively suppressing high-frequency components above 150 Hz. The FFT plots confirm these findings, showing that the Butterworth filter exhibits a sharper cutoff and greater retention of dominant frequency bands around 30–80 Hz compared to the Kalman filter. This supports the SNR analysis results, in which the Butterworth filter achieved higher enhancement levels under the same testing conditions.

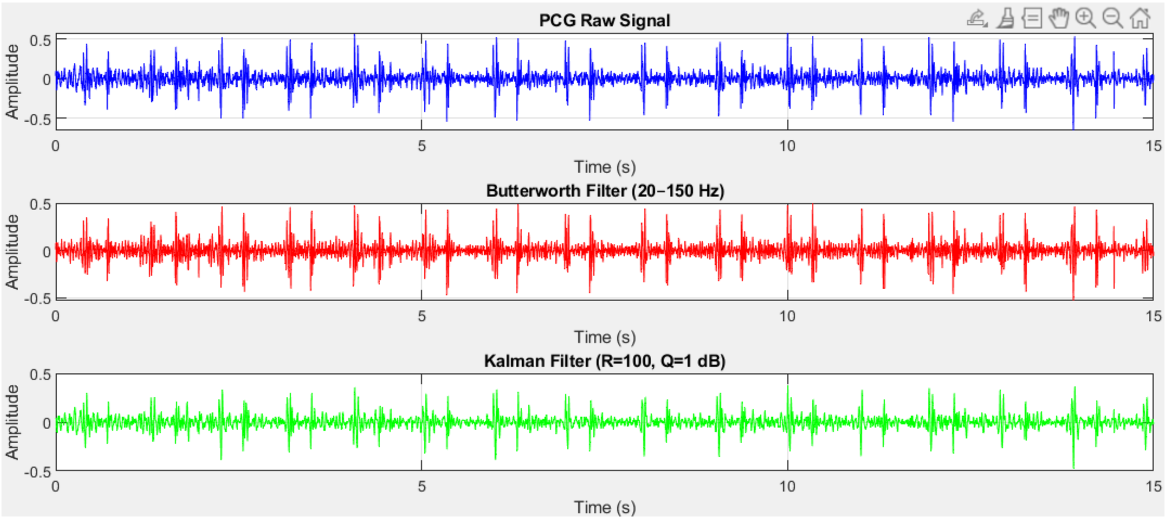

Figure 5. Time-domain comparison of PCG: Butterworth preserves S1–S2; Kalman smooths with attenuation

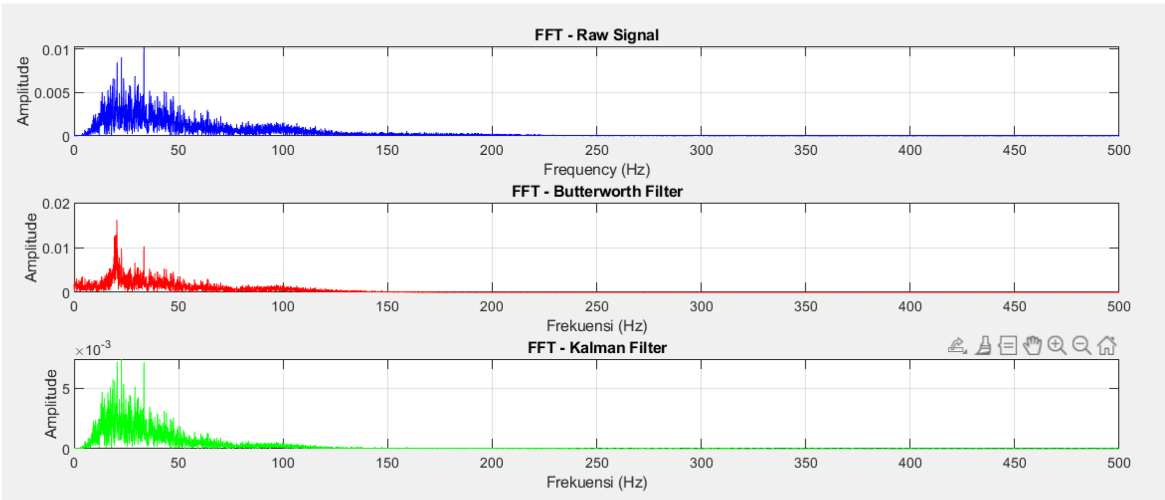

Figure 6. FFT comparison: Butterworth suppresses >150 Hz; Kalman reduces noise with slight attenuation

3.1.1. Kalman filter results

As shown in Table 1, after the filtering process was performed, the SNR values for 15 heart sound signals were measured after being filtered using the Kalman digital filter. The measurement results showed the SNR values for all heart sound signals after the filtering process was conducted with the Kalman digital filter according to the magnitude of the coefficients applied. The Kalman filter tests were performed on 15 mannequin heart sound signals with a normal sinus rhythm. Each of the 15 signals was then filtered using digital Kalman filters with different coefficient values, namely R: 100 and Q: 1, R: 10 and Q: 1, R: 1 and Q:1, and R: 1 and Q: 0.1.

Table 1. SNR results of 15 mannequin signals after being filtered with the Kalman filter

Mannequin signal	Kalman filter SNR Value R:100; Q:1 (dB)	Kalman filter SNR Value R:10; Q:1 (dB)	Kalman filter SNR Value R:1; Q:1 (dB)	Kalman filter SNR Value R:1; Q:0,1 (dB)
1	20.043	19.264	19.040	19.253
2	19.618	18.832	18.630	18.822
3	19.740	19.189	19.016	19.178
4	21.237	20.792	20.605	20.778
5	21.600	21.274	21.099	21.257
6	20.424	19.835	19.630	19.820
7	20.746	20.210	20.016	20.195
8	20.416	19.803	19.597	19.789
9	20.397	20.061	19.908	20.046
10	20.374	20.154	20.025	20.138
11	19.544	19.162	19.015	19.150
12	21.746	21.782	21.677	21.760
13	21.533	21.520	21.418	21.500
14	21.242	21.348	21.262	21.327
15	23.569	23.888	23.818	23.856
Mean	**20.815**	**20.474**	**20.317**	**20.458**

Based on the average values obtained in Table 1, the SNR values were arranged according to the Kalman filter coefficient settings as follows: R: 100 and Q: 1 with an average SNR value of 20.815 dB, R: 10, and Q: 1 with an average SNR value of 20,474 dB, R: 1, and Q: 1 with an average SNR value of 20.317 dB and coefficient values of R: 1 and Q: 0.1 with an average SNR value of 20.458 dB (Figure 7).

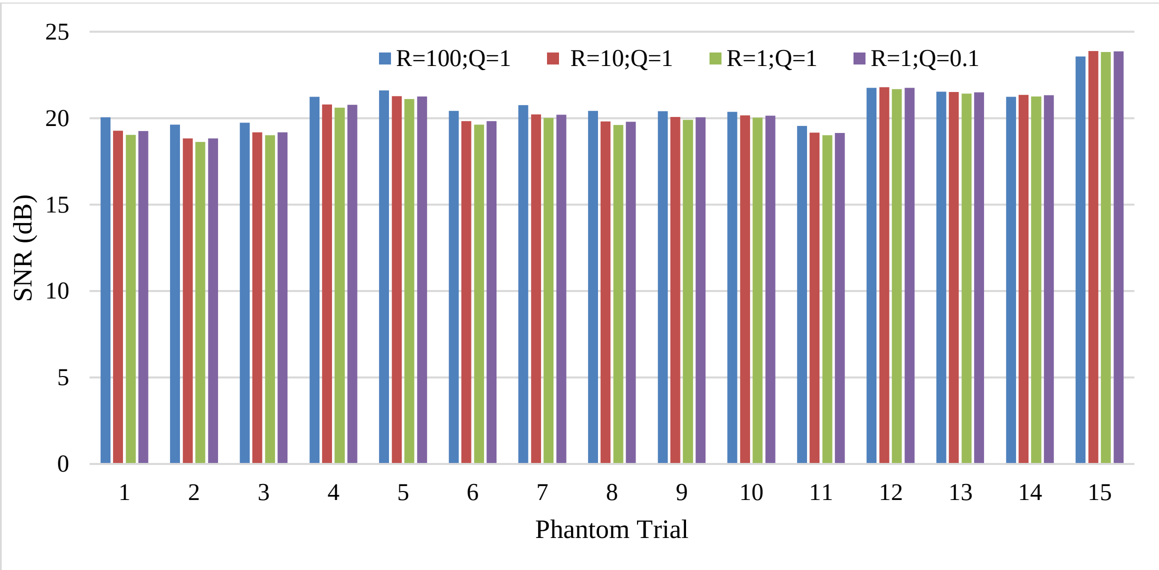

Figure 7. SNR (dB) for different R and Q parameter

3.1.2. Butterworth band-pass filter results

Based on Table 2, after the filtering process was performed, the SNR values for 17 heart sound signals were measured before and after being filtered using a Butterworth band-pass digital filter. The measurement results showed the SNR values for all heart sound signals after the filtering process using the Butterworth band-pass digital filter according to the given filter order. The testing of the digital Butterworth band-pass filter was carried out using 15 mannequin heart sound signals with a normal sinus rhythm. Among these 15 mannequin heart sound signals, they were filtered by a digital Butterworth band-pass filter with different orders, namely 2, order 4, order 6, and order 8. Based on the average values obtained in Table 2, the SNR values were arranged as follows: band-pass filter order 8 with an average SNR value of 25.659 dB, order 6 with an average SNR value of 25.585 dB, order 4 with an average SNR value of 25.362 dB, and order 2 with an average SNR value of 24,590 dB. These results are also illustrated in the FFT visualization for each filter order (Figure 8).

Table 2. SNR results of 15 mannequin signals after being filtered with the Butterworth band-pass filter

Mannequin signal	Band-pass filter SNR (order 2) (dB)	Band-pass filter SNR (order 4) (dB)	Band-pass filter SNR (order 6) (dB)	Band-pass filter SNR (order 8) (dB)
1	23.231	24.227	24.658	24.857
2	24.289	24.833	24.833	25.068
3	23.627	24.706	25.101	25.251
4	24.477	25.306	25.551	25.609
5	24.794	25.548	25.758	25.791
6	23.780	24.793	25.181	25.333
7	24.115	25.061	25.395	25.502
8	23.793	24.781	25.165	25.319
9	24.561	25.361	25.616	25.691
10	24.872	25.578	25.771	25.811
11	24.289	25.199	25.496	25.579
12	25.599	26.148	26.237	26.207
13	25.534	26.077	26.149	26.149
14	25.766	26.255	26.309	26.261
15	26.130	26.561	26.555	26.462
Mean	**24.590**	**25.362**	**25.585**	**25.659**

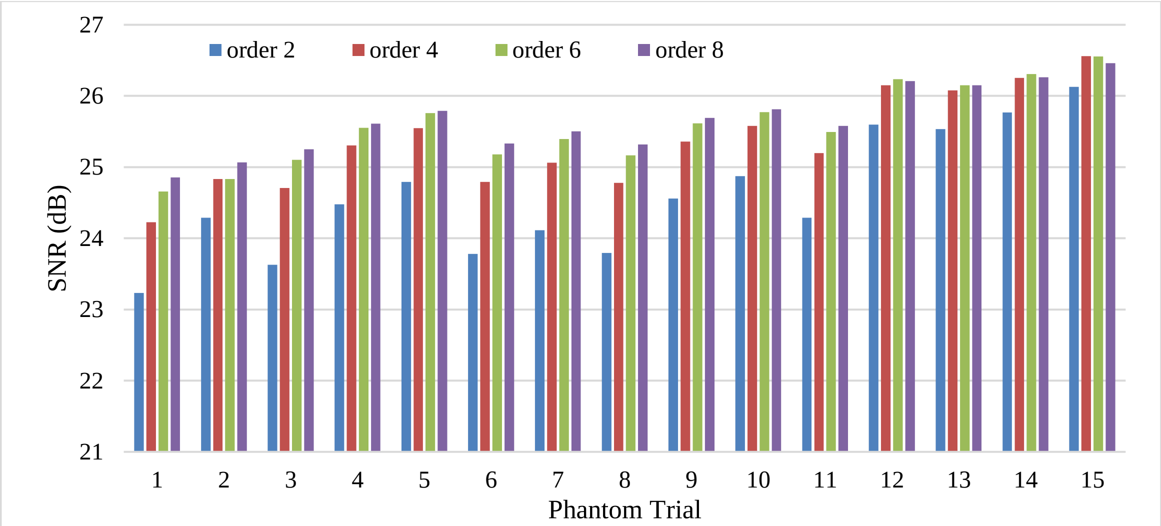

Figure 8. SNR (dB) for different orde

3.1.3. Statistical analysis of filter performance

To evaluate whether variations in filter parameters significantly affected the SNR, a one-way analysis of variance (ANOVA) was performed for both filtering methods. For the Kalman filter, the ANOVA results showed an F-statistic of 0.414 with a p-value of 0.743, indicating no significant difference in SNR among the tested R and Q coefficient configurations. This suggests that within the examined range, changes in these coefficients do not significantly influence SNR enhancement. For the Butterworth band-pass filter, the ANOVA yielded an F-statistic of 8.437 and a p-value of 0.00010, demonstrating a statistically significant effect of filter order on SNR improvement. A subsequent Tukey HSD post-hoc test revealed that filters with higher orders (4^{th}, 6^{th}, and 8^{th}) produced significantly higher SNR values compared to the 2^{nd}-order configuration ($p<0.05$). However, differences among the higher-order filters (4^{th} vs. 6^{th} vs. 8^{th}) were not statistically significant ($p>0.05$), suggesting that increasing the order beyond four does not yield additional measurable gains. These results indicate that the Butterworth filter's order parameter significantly influences noise suppression and signal clarity, whereas the Kalman filter's R and Q parameters exhibit more stable but less sensitive SNR performance across parameter variations.

3.2. Discussion

In the Kalman filter, the configuration with higher coefficient values (R:100, Q:1) achieved the highest average SNR of 20.815 dB, followed by R:10, Q:1 and R:1, Q:0.1, with SNR values of 20.474 dB and 20.458 dB, respectively. The lowest SNR was obtained with R:1, Q:1 (20.317 dB). Larger R coefficients improve signal stability by emphasizing measurement accuracy, although excessively high values can over smooth the waveform and reduce amplitude detail. For the Butterworth digital band-pass filter, higher orders produced better noise suppression and clearer heart sound signals. The 8^{th}-order configuration achieved the highest average SNR (25.659 dB), followed by the 6^{th} (25.585 dB) and 4^{th} (25.362 dB) orders, while the 2^{nd} order provided the lowest improvement (24.590 dB). Increasing the order improves passband selectivity and removes unwanted frequencies more effectively, thereby enhancing the PCG waveform quality within the 20–150 Hz range that contains the main S1–S2 components.

The statistical analysis supports these findings. The one-way ANOVA showed no significant difference in SNR among Kalman coefficient settings (p=0.743), indicating stable but less sensitive performance. In contrast, the Butterworth filter showed a significant effect of order on SNR (F=8.437, p=0.00010). Tukey post-hoc results confirmed that SNR increased significantly from the 2^{nd} to the 4^{th} order, while higher orders provided no further statistical benefit (p>0.05). Thus, a 4^{th}–6^{th} order Butterworth filter provides an optimal balance between computational efficiency and noise reduction accuracy.

The performance differences between the two filters reflects their underlying principles. The Kalman filter estimates the true signal through recursive state modeling and adapts dynamically to noise characteristics, making it suitable for nonstationary environments. Meanwhile, the Butterworth filter operates in the frequency domain, offering a maximally flat response in the passband and efficient suppression of frequencies beyond 150 Hz. The Butterworth design is simpler and more predictable for fixed-frequency biomedical applications, whereas the Kalman filter provides adaptive flexibility under changing conditions.

From an electrical engineering perspective, both algorithms can be effectively implemented on embedded systems such as ESP32, STM32, or Arduino. The Butterworth filter’s low complexity allows real-time processing using IIR structures with minimal computational cost. Although the Kalman filter requires heavier computation, it can be optimized using fixed-point arithmetic or lightweight recursive matrices, making it feasible for adaptive filtering in low-power biomedical devices. These results align with previous studies highlighting the integration of digital filters into microcontroller-based bio signal systems for real-time enhancement [28], [29]. Implementing these algorithms in embedded firmware would enable real-time filtering and denoising of PCG signals without relying on MATLAB or PC-based computation, thereby improving portability and efficiency [30]-[32].

From an informatics viewpoint, the ESP32 platform provides wireless connectivity via Wi-Fi and Bluetooth, allowing filtered heart sound data to be transmitted to hospital servers or mobile applications in real time. Storing filtered PCG data in standardized formats such as CSV, EDF, or HL7 ensures compatibility with electronic medical record (EMR) systems. This capability supports telemedicine applications and long-term cardiac monitoring, facilitating integration into digital healthcare infrastructures [33].

However, several limitations remain. The Bluetooth output currently transmits unfiltered audio, and filtering was performed offline in MATLAB. Future integration directly into the ESP32 firmware will enable true real-time operation. Automatic beats per minute (BPM) detection have not yet been implemented, and analog front-end conditioning (PSC) may be needed to stabilize condenser microphone input signals. Moreover, benchmarking against commercial stethoscopes and AI-based enhancement methods have not yet been performed. Comparative evaluation with systems such as Littmann Core or Eko DUO and machine-learning-based denoising algorithms would strengthen clinical relevance and validate professional-level performance. Although this study focused only on heart sound (PCG) signals from mannequins with normal sinus rhythm, future work should extend testing to other biomedical sound types such as lung or vascular sounds to evaluate generalization capability. Comparing SNR improvements across multiple signal modalities will enhance the robustness of the proposed method for multi-organ auscultation systems.

Overall, the findings confirm that higher-order Butterworth filters achieve superior SNR enhancement and waveform preservation, making them ideal for low-cost, real-time embedded applications. The Kalman filter, while yielding slightly lower SNR, provides adaptability in dynamically changing noise environments. Combining both (using Butterworth filtering for baseline denoising followed by Kalman-based adaptive smoothing) could yield more stable and noise-resilient performance in future designs. Future research will focus on embedding these filters directly into ESP32 firmware, integrating AI-based classification for cardiac anomaly detection, and validating system performance using human-subject data. With these advancements, the proposed system can evolve into an efficient, connected, and clinically applicable digital stethoscope within modern biomedical informatics and telehealth frameworks.

4. CONCLUSION

The purpose of this study was to develop and evaluate an electronic stethoscope system using a condenser microphone sensor to detect mannequin heart sounds with normal sinus rhythm and to investigate the effectiveness of two digital filtering methods (the Kalman filter and the Butterworth band-pass filter) in enhancing signal quality. The key finding from this investigation is that the 8th-order Butterworth band-pass filter achieved the highest SNR performance with an average value of 25.659 dB, while the best Kalman filter configuration (R:100, Q:1) produced an average SNR value of 20.815 dB. These results confirm that the frequency-selective Butterworth approach provides more effective noise suppression than the recursive estimation technique of the Kalman filter. In summary, the condenser microphone sensor successfully detected mannequin heart sounds, the Butterworth band-pass filter consistently outperformed the Kalman filter across all tested parameters, and the filter's order or coefficient selection significantly influenced the output SNR. It is recommended that future research focus on integrating real-time digital filtering within the ESP32 firmware, incorporating automatic pulse rate (BPM) detection, benchmarking against commercial and AI-based filtering systems, and validating the system using human-subject data to enhance clinical applicability and diagnostic reliability.

ACKNOWLEDGMENTS

The authors would like to express their deepest gratitude to the Department of Electromedical Engineering, Poltekkes Kemenkes Surabaya, for providing the research facilities and support throughout this study. Special thanks are extended to all lecturers and laboratory staff who assisted during the experimental setup and data collection process. The authors also acknowledge the collaboration with the Department of Computer Engineering, Azerbaijan State Oil and Industry University, Baku, Azerbaijan, for their valuable insights and international cooperation, which enhanced the quality of this study. This study was conducted as part of the institutional research program of Poltekkes Kemenkes Surabaya, and the authors sincerely appreciate the continuous encouragement and resources provided by the institution.

FUNDING INFORMATION

This study was funded by Poltekkes Kemenkes Surabaya through an institutional research grant. The authors gratefully acknowledge the financial support provided by the institution, which made this study possible.

AUTHOR CONTRIBUTIONS STATEMENT

This journal uses the Contributor Roles Taxonomy (CRediT) to recognize individual author contributions, reduce authorship disputes, and facilitate collaboration.

Name of Author	C	M	So	Va	Fo	I	R	D	O	E	Vi	Su	P	Fu
Endang Dian Setioningsih	✓								✓					
Sumber		✓								✓				
Triwiyanto					✓					✓				
Vugar Abdullayev						✓			✓					
Farid Amrinsani	✓								✓					
Bima Maulana Raharjo						✓			✓					
Tetrik Fa'altin		✓								✓				

C : **C**onceptualization
M : **M**ethodology
So : **So**ftware
Va : **Va**lidation
Fo : **Fo**rmal analysis
I : **I**nvestigation
R : **R**esources
D : **D**ata Curation
O : Writing - **O**riginal Draft
E : Writing - Review & **E**diting
Vi : **Vi**sualization
Su : **Su**pervision
P : **P**roject administration
Fu : **Fu**nding acquisition

CONFLICT OF INTEREST STATEMENT

The authors declare that there are no conflicts of interest regarding the publication of this paper. The authors confirm that there are no financial, personal, or institutional relationships that could have influenced the work reported in this study.

INFORMED CONSENT

Written informed consent was obtained from all participants prior to their inclusion in this study. Each participant received a comprehensive explanation regarding the study objectives, procedures, potential risks, and expected benefits, and was informed of their right to withdraw at any time without consequence.

All data were collected and processed in accordance with applicable ethical standards and regulations, and participant confidentiality and anonymity were strictly maintained throughout the study. For participants whose data are presented in identifiable form, explicit consent for publication was additionally obtained.

ETHICAL APPROVAL

This study was reviewed and approved by the Health Research Ethics Committee of Poltekkes Kemenkes Surabaya (KEPK Poltekkes Surabaya) under approval number No. EA/1246/KEPK-Poltekkes_Sby/V/2024. All research procedures were conducted in accordance with applicable ethical guidelines and regulations, including principles outlined in the Declaration of Helsinki.

DATA AVAILABILITY

The data that support the findings of this study are available from the corresponding author, [initials: ED], upon reasonable request.

REFERENCES

[1] R. D. Ayu and N. Adnan, "Risk of Hypertension in the Incidence of Coronary Heart Disease in Urban and Rural Communities Indonesia (Longitudinal Analysis of IFLS 2007-2014)," *Jurnal Ilmu Kesehatan Masyarakat*, vol. 11, no. 2, pp. 171–184, Jul. 2020, doi: 10.26553/jikm.2020.11.2.171-184.

[2] T. Suryati and S. Suyitno, "Prevalence And Risk Factors Of The Ischemic Heart Diseases In Indonesia: A Data Analysis Of Indonesia Basic Health Research (Riskesdas) 2013," *Public Health of Indonesia*, vol. 6, no. 4, pp. 138–144, Dec. 2020, doi: 10.36685/phi.v6i4.366.

[3] A. V. Poznyak *et al.*, "Hypertension as a risk factor for atherosclerosis: Cardiovascular risk assessment," *Frontiers in Cardiovascular Medicine*, vol. 9, 2022, doi: 10.3389/fcvm.2022.959285.

[4] R. A. S. Faulata, A. D. Laksono, and R. D. Wulandari, "Heart Disease in Indonesia in 2018: An Ecological Analysis," *Indian Journal of Forensic Medicine & Toxicology*, vol. 15, no. 3, pp. 3927–3933, May 2021, doi: 10.37506/ijfmt.v15i3.15910.

[5] A. Groenewegen, F. H. Rutten, A. Mosterd, and A. W. Hoes, "Epidemiology of heart failure," *European Journal of Heart Failure*, vol. 22, no. 8, pp. 1342–1356, Aug. 2020, doi: 10.1002/ejhf.1858.

[6] S. Ashiq and K. Ashiq, "Genetic Perspective of The Congenital Heart Disease," *Pakistan Heart Journal*, vol. 53, no. 3, Nov. 2020, doi: 10.47144/phj.v53i3.1982.

[7] B. Omarov, A. Batyrbekov, A. Suliman, B. Omarov, Y. Sabdenbekov, and S. Aknazarov, "Electronic stethoscope for detecting heart abnormalities in athletes," in *2020 21st International Arab Conference on Information Technology (ACIT)*, IEEE, Nov. 2020, pp. 1–5, doi: 10.1109/ACIT50332.2020.9300109.

[8] R. Bharti, A. Khamparia, M. Shabaz, G. Dhiman, S. Pande, and P. Singh, "Prediction of Heart Disease Using a Combination of Machine Learning and Deep Learning," *Computational Intelligence and Neuroscience*, vol. 2021, no. 1, Jan. 2021, doi: 10.1155/2021/8387680.

[9] V. Kumar *et al.*, "Auscultation of heart, its changes and impacts on the cardiac pathophysiology: A descriptive review.," *Asian Journal of Research in Pharmaceutical Sciences*, pp. 149–154, May 2024, doi: 10.52711/2231-5659.2024.00023.

[10] R. S. Vasudevan *et al.*, "Persistent Value of the Stethoscope in the Age of COVID-19," *The American Journal of Medicine*, vol. 133, no. 10, pp. 1143–1150, Oct. 2020, doi: 10.1016/j.amjmed.2020.05.018.

[11] J. K. Roy, T. S. Roy, and S. C. Mukhopadhyay, "Heart Sound: Detection and Analytical Approach Towards Diseases," *Modern Sensing Technologies*, pp. 103–145, 2019, doi: 10.1007/978-3-319-99540-3_7.

[12] M. Yildirim, "Diagnosis of Heart Diseases Using Heart Sound Signals with the Developed Interpolation, CNN, and Relief Based Model," *Traitement du Signal*, vol. 39, no. 3, pp. 907–914, Jun. 2022, doi: 10.18280/ts.390316.

[13] A. Yadav, A. Singh, M. K. Dutta, and C. M. Travieso, "Machine learning-based classification of cardiac diseases from PCG recorded heart sounds," *Neural Computing and Applications*, vol. 32, no. 24, pp. 17843–17856, Dec. 2020, doi: 10.1007/s00521-019-04547-5.

[14] S. Ogawa, F. Namino, T. Mori, G. Sato, T. Yamakawa, and S. Saito, "AI diagnosis of heart sounds differentiated with super StethoScope," *Journal of Cardiology*, vol. 83, no. 4, pp. 265–271, Apr. 2024, doi: 10.1016/j.jjcc.2023.09.007.

[15] S. Khoruamkid and S. Visitsattapongse, "A Low-Cost Digital Stethoscope for Normal and Abnormal Heart Sound Classification," in *2022 14th Biomedical Engineering International Conference (BMEiCON)*, IEEE, Nov. 2022, pp. 1–6, doi: 10.1109/BMEiCON56653.2022.10012113.

[16] L. J. Chagas *et al.*, "Electronic Stethoscopes in The Diagnosis of Heart Disorders: An Integrative Review of The Evidence And Clinical Applications," *International Journal of Health Science*, vol. 4, no. 73, pp. 2–6, Aug. 2024, doi: 10.22533/at.ed.1594732405087.

[17] R. Prawira, S. Ismail, A. Johan, and R. Ismail, "Description of the usefulness and ease of use wireless stethoscope for auscultation: A pilot study," *JNKI (Jurnal Ners dan Kebidanan Indonesia) (Indonesian Journal of Nursing and Midwifery)*, vol. 10, no. 4, p. 321, Jan. 2023, doi: 10.21927/jnki.2022.10(4).321-329.

[18] Y.-C. Wu *et al.*, "Development of an Electronic Stethoscope and a Classification Algorithm for Cardiopulmonary Sounds," *Sensors*, vol. 22, no. 11, p. 4263, Jun. 2022, doi: 10.3390/s22114263.

[19] M. Zhang, M. Li, L. Guo, and J. Liu, "A Low-Cost AI-Empowered Stethoscope and a Lightweight Model for Detecting Cardiac and Respiratory Diseases from Lung and Heart Auscultation Sounds," *Sensors*, vol. 23, no. 5, p. 2591, Feb. 2023, doi: 10.3390/s23052591.

[20] B. Zhu, Z. Zhou, S. Yu, X. Liang, Y. Xie, and Q. Sun, "Review of Phonocardiogram Signal Analysis: Insights from the PhysioNet/CinC Challenge 2016 Database," *Electronics (Basel)*, vol. 13, no. 16, p. 3222, Aug. 2024, doi: 10.3390/electronics13163222.

[21] P. C. Nugraha *et al.*, "Exploration of digital filters on cardiac monitor devices equipped with non-invasive blood pressure (NIBP)," *Indonesian Journal of Electronics, Electromedical Engineering, and Medical Informatics*, vol. 6, no. 4, pp. 252–263, 2024, doi: 10.35882/edd73780.
[22] J. Malwade, S. Sayyed, J. Nasir, Y. Parab, G. Narayanan, and S. Gupta, "Wireless Stethoscope with Bluetooth Technology," in *2020 International Conference on Computational Performance Evaluation (ComPE)*, Jul. 2020, pp. 168–172, doi: 10.1109/ComPE49325.2020.9200163.
[23] S. E. Kjeldsen, "Hypertension and cardiovascular risk: General aspects," *Pharmacological Research*, vol. 129, pp. 95–99, Mar. 2018, doi: 10.1016/j.phrs.2017.11.003.
[24] C. T. Somefun, S. A. Daramola, and T. E. Somefun, "Advancements and Applications of Adaptive Filters in Signal Processing," *Journal Européen des Systèmes Automatisés*, vol. 57, no. 5, pp. 1259–1272, Oct. 2024, doi: 10.18280/jesa.570502.
[25] Y. Chen, Y. Zheng, S. Johnson, R. Wiffen, and B. Yang, "A comparative study of accuracy in major adaptive filters for motion artifact removal in sleep apnea tests," *Medical & Biological Engineering & Computing*, vol. 62, no. 3, pp. 829–842, Mar. 2024, doi: 10.1007/s11517-023-02979-9.
[26] P. Oktivasari *et al.*, "Modeling Data Set of Indonesian Heart Sound Signals," in *2024 7th International Conference of Computer and Informatics Engineering (IC2IE)*, IEEE, Sep. 2024, pp. 1–7, doi: 10.1109/IC2IE63342.2024.10748187.
[27] M. S. Nazemi, H. Hakimnejad, and Z. Azimifar, "PCG denoising using AR-based Kalman Filter," in *2021 29th Iranian Conference on Electrical Engineering (ICEE)*, IEEE, May 2021, pp. 902–906, doi: 10.1109/ICEE52715.2021.9544365.
[28] J. Gonzalez, E. Galvis, and C. Velandia, "Implementation of real-time filter using an open-source platform oriented to R-wave detection," in *2016 XXI Symposium on Signal Processing, Images and Artificial Vision (STSIVA)*, IEEE, Aug. 2016, pp. 1–5, doi: 10.1109/STSIVA.2016.7743351.
[29] H. R. Mahmood, M. K. Hussein, and R. A. Abedraba, "Development of Low-Cost Biosignal Acquisition System for ECG, EMG, and EOG," *Wasit Journal of Engineering Sciences*, vol. 10, no. 3, pp. 191–202, Dec. 2022, doi: 10.31185/ejuow.Vol10.Iss3.352.
[30] A. F. Rohman, M. R. Mak'ruf, T. Triwiyanto, L. Lamidi, and P.-H. Huynh, "Analysis of the Effectiveness of Using Digital Filters in Electronic Stethoscopes," *Journal of Electronics, Electromedical Engineering, and Medical Informatics*, vol. 4, no. 4, Oct. 2022, doi: 10.35882/jeeemi.v4i4.256.
[31] H. Fauzi, A. Rizal, M. 'Aqila, A. Oktarianto, and Z. Said, "Classification of Normal and Abnormal Heart Sounds Using Empirical Mode Decomposition and First Order Statistic," *Journal of Electronics, Electromedical Engineering, and Medical Informatics*, vol. 5, no. 2, pp. 82–88, Apr. 2023, doi: 10.35882/jeeemi.v5i2.287.
[32] A. Triwerdani, S. Syaifudin, B. Utomo, and A. Basit, "Mechanical Fetal Simulator for Fetal Doppler Testing," *Journal of Electronics, Electromedical Engineering, and Medical Informatics*, vol. 4, no. 2, pp. 84–88, Apr. 2022, doi: 10.35882/jeeemi.v4i2.5.
[33] Md. R. R. Akash and K. Shikder, "IoT Based Real Time Health Monitoring System," in *2020 Research, Innovation, Knowledge Management and Technology Application for Business Sustainability (INBUSH)*, IEEE, Feb. 2020, pp. 167–171, doi: 10.1109/INBUSH46973.2020.9392163.

BIOGRAPHIES OF AUTHORS

Endang Dian Setioningsih completed her graduate studies (M.Eng.) in Electrical Engineering at the Sepuluh Nopember Institute of Technology, Surabaya, in 2010. She is a lecturer teaching Physics and Therapeutic Equipment courses in the Applied Undergraduate Study Program in Electromedical Technology Engineering, Department of Electromedical Technology, Health Polytechnic, Ministry of Health, Surabaya. Her Tridarma activities include community service and research. Her current research focuses on wireless electronic stethoscopes, particularly on transmitting sound signals and applying digital filters to improve system performance. She is also an active member of Indonesian Electromedical Association (IKATEMI), which aims to enhance the professionalism of Electromedical and Medical Technology technicians in Indonesia. In addition, she currently serves as an administrator of Indonesian Electromedical Personnel Education Association (APTEMI). She can be contacted at email: dian18@poltekkesdepkes-sby.ac.id.

Sumber completed his master's degree (M.Eng.) in Engineering Physics at the Sepuluh Nopember Institute of Technology, Surabaya, from 2012 to 2014. He is a lecturer in diagnostics, electrical installations, and discrete electronics practicum at the Department of Electromedical Technology, Health Polytechnic, Ministry of Health, Surabaya. His Tridarma activities include community service and research. His current research involves analyzing the effectiveness of digital filters in electronic stethoscopes using a condenser microphone sensor to diagnose heart conditions through detected heart sounds. He is also an active member of Indonesian Electromedical Association (IKATEMI), which aims to enhance the professionalism of Electromedical and Medical Technology technicians in Indonesia. He can be contacted at email: sumber72@poltekkesdepkes-sby.ac.id.

Dr. Triwiyanto received his B.S. degree in Physics from Airlangga University, Indonesia; his M.S. degree in Electronic Engineering from the Institut Teknologi Sepuluh Nopember, Surabaya, Indonesia, in 2004; and his Ph.D. degree in Electrical Engineering from Gadjah Mada University, Yogyakarta, Indonesia, in 2018. From 1998 to 2004, he served as a Senior Lecturer in the Microcontrollers Laboratory. Since 2005, he has been working as an Assistant Professor in the Department of Medical Electronics Technology, Health Polytechnic, Ministry of Health, Surabaya, Indonesia. In 2018, he received the Best Doctoral Student award from Gadjah Mada University. Additionally, he serves as Editor-in-Chief for several peer-reviewed journals and as Chairman or Technical Program Committee member in various international conferences. His research interests include microcontrollers, electronics, biomedical signal processing, machine learning, rehabilitation engineering, and surface electromyography (sEMG)-based physical human–robot interaction. He can be contacted at email: triwiyanto123@gmail.com.

Vugar Abdullayev, Ph.D. was born in Azerbaijan. He received his B.S. degree in Automatics and Control of Technical Systems and his M.S. degree in Manufacturing Automation and Informatics from the Azerbaijan State Oil and Industry University (ASOIU), Baku, Azerbaijan, in 2000, and his Ph.D. degree from the Institute of Cybernetics, Azerbaijan National Academy of Sciences, in 2005. From 2002 to 2004, he worked as an IT and Payment Systems expert at the Central Bank of Azerbaijan. From 2004 to 2012, he served as a Researcher and Head Researcher at the Institute of Cybernetics, Azerbaijan National Academy of Sciences. Since 2012, he has been an Associate Professor and Doctor of Technical Sciences at the Department of Computer Engineering, Azerbaijan State Oil and Industry University. He is the author of 85 scientific papers and has published 20 book chapters and 10 edited books (Taylor & Francis) in the healthcare ecosystem. His research interests include cyber-physical systems, IoT, big data, smart cities, information technologies, cloud computing, computational complexity, machine learning (artificial intelligence), and behavioral science computing. He can be contacted at email: abdulvugar@mail.ru.

Farid Amrinsani completed the Diploma III and Diploma IV programs in Electromedical Technology and later obtained a Master of Applied Engineering degree in Electrical Engineering from the Surabaya State Electronics Polytechnic. He serves as an academic staff member specializing in basic electronics and programmable devices at the Department of Electromedical Technology, Health Polytechnic, Ministry of Health, Surabaya. His Tridarma activities include community service and research. He is also an active administrator of IKATEMI (Indonesian Electromedical Association), which aims to improve the professionalism of Electromedical and Medical Technology technicians in Indonesia. He can be contacted at email: far@poltekkesdepkes-sby.ac.id.

Bima Maulana Raharjo is a graduate of the Applied Electromedical Engineering program at the Health Polytechnic, Ministry of Health, Surabaya (2019–2023). He currently works as an Electromedical Technician in the East and North Kalimantan regions at PT Tawada Health Services. He can be contacted at email: bimamaulana1234@gmail.com.

Tetrik Fa'altin is a student at the Health Polytechnic, Ministry of Health, Surabaya, Department of Electromedical Technology, Applied Undergraduate Program in Electromedical Engineering Technology. She is currently in her third year of study. In addition to her studies, she is active in student organizations and works as a teaching assistant. She is grateful for the opportunity to contribute to this research. She can be contacted at email: tetrikfaaltin@gmail.com.